Video Article

# Isolation of Intact, Whole Mouse Mammary Glands for Analysis of Extracellular Matrix Expression and Gland Morphology

Christopher Thompson[1], Katherine Keck[2], Abigail Hielscher[2]

[1]Department of Biochemistry and Molecular Biology, University of Nebraska Medical Center

[2]Department of Biomedical Sciences, GA-PCOM

Correspondence to: Abigail Hielscher at abigailhi@pcom.edu

URL: https://www.jove.com/video/56512
DOI: doi:10.3791/56512

Keywords: Physiology, Issue 128, Extracellular matrix, mammary glands, ducts, immunohistochemistry

Date Published: 10/30/2017

Citation: Thompson, C., Keck, K., Hielscher, A. Isolation of Intact, Whole Mouse Mammary Glands for Analysis of Extracellular Matrix Expression and Gland Morphology. *J. Vis. Exp.* (128), e56512, doi:10.3791/56512 (2017).

## Abstract

The goal of this procedure was to harvest the #4 abdominal mammary glands from female nulliparous mice in order to assess ECM expression and ductal architecture. Here, a small pocket below the skin was created using Mayo scissors, allowing separation of the glands within the subcutaneous tissue from the underlying peritoneum. Visualization of the glands was aided by the use of 3.5x-R surgical micro loupes. The pelt was inverted and pinned back allowing identification of the intact mammary fat pads. Each of the #4 abdominal glands was bluntly dissected by sliding the scalpel blade laterally between the subcutaneous layer and the glands. Immediately post-harvest, glands were placed in 10% neutral buffered formalin for subsequent tissue processing. Excision of the entire gland is advantageous because it primarily eliminates the risk of excluding important tissue-wide interactions between ductal epithelial cells and other microenvironmental cellular populations that could be missed in a partial biopsy. One drawback of the methodology is the use of serial sections from fixed tissues which limits analyses of ductal morphogenesis and protein expression to discrete locations within the gland. As such, changes in ductal architecture and protein expression in 3 dimensions (3D) is not readily obtainable. Overall, the technique is applicable to studies requiring whole intact murine mammary glands for downstream investigations such as developmental ductal morphogenesis or breast cancer.

## Video Link

The video component of this article can be found at https://www.jove.com/video/56512/

## Introduction

Breast cancer is characterized by a substantial degree of tissue fibrosis[1,2,3,4]. Referred to as the ECM, this non-cellular entity is found in varying degrees in all tissues and is primarily comprised of a complex meshwork of fibrillar and non-fibrillar collagens, elastin, and glycoproteins in addition to various signaling molecules that are sequestered in this matrix. Under homeostatic conditions, the deposition and degradation of the ECM is tightly controlled.[5] During breast tumorigenesis, the balance of ECM deposition and degradation is disrupted. As such, breast tumors have been reported to express abundant ECM proteins such as collagens, fibronectin and tenascin-C amongst others.[6] The abnormal expression of these proteins in addition to increased patterns of matrix crosslinking has been documented to promote breast tumor progression, metastasis and therapy resistance[1,3,4,7,8,9].

To assess ECM composition and ductal morphology, isolation of intact mammary glands was performed. Here, we used female nulliparous mice deficient for caveolin-1, an integral membrane protein which has been linked to an aggressive breast tumor signature[10,11,12], and control female nulliparous B6 mice. Histological processing and staining of these tissues permitted the identification of several ECM proteins along with characterization of ductal morphology.

Overall, the isolation of whole, intact mammary glands gives researchers the opportunity to investigate tissue-wide morphological or cellular changes occurring in response to exogenous or endogenous factors. Drawbacks of the technique are associated with analyses of 2 dimension (2D) tissue sections as opposed to a 3D perspective, which would yield a more complete picture of the complex morphology of the ductal tree. Given the complexity of cell-cell and cell-ECM interactions that take place in the mammary gland, the isolation of whole, intact glands is advantageous for efficiently analyzing ductal morphology and protein expression in various regions of the murine mammary gland.

## Protocol

Procedures involving animal subjects in this protocol were reviewed and approved by the Institutional Animal Care and Use Committee of the Philadelphia College of Osteopathic Medicine and all techniques were conducted under strict ethical guidelines.

## 1. Sample Procurement and Processing

1. Select appropriate animal subject and place into a $CO_2$ chamber. For this experiment, use 8-10 week old female nulliparous B6.Cg-Cav1tmMls/J and C57Bl/6J.
2. Turn on gas flow to 30-40%. Once the animal is visibly unconscious after about 2 min, open the gas valve to full pressure for an additional 5 min.
   NOTE: Confirm animal death by observing visible signs of breathing (*e.g.* movement of the chest) for a period of 10 min after cessation of $CO_2$ delivery. If the animal is still alive, it may be placed back in the $CO_2$ chamber. Cervical dislocation may also be used although it is not recommended as blood may accumulate around the mammary glands interfering with the dissection and results.
3. Following sacrifice, pin carcass in a supine position and saturate with 70% ethanol.
4. Pinch the pelt just above the pubis using forceps and nick with small surgical scissors. Rotating the scissors, cut the pelt along the ventral midline moving caudal to cranial.
5. With larger scissors or a hemostat, bluntly dissect the subcutaneous fascia bilaterally, using caution not to puncture the peritoneum. Cut along the horizontal margins at both distal ends of the incision.
6. Pin the pelt flaps open and spray again with 70% ethanol.
   NOTE: Although the use of 70% ethanol permitted better visual distinction between the gland and the surrounding subcutaneous tissue, be careful to avoid drying of the tissue as a result of use of this solution. To avoid drying, remove the gland in a time frame not to exceed 4 min. As an alternative to 70% ethanol, the investigator may also substitute a general isolate buffer, such as 1x PBS, to avoid tissue desiccation.
7. Locating the mammary glands of interest, slide a #4 scalpel blade along the inside of the pelt flaps, cutting the mammary gland and associated cutaneous adipose free from the dermis.
   NOTE: 3.5x surgical micro loupes may aid in easier visualization of the glands.
8. Immediately submerge newly isolated gland in conical tube containing 10:1 solution-tissue volume of 10% neutral buffered formalin for 24-48 h.
   NOTE: Depending on intent of study, many alternative fixatives may be used such as paraformaldehyde, ethanol for genomic studies, and commercially available RNA preserving buffers.
9. Follow institutional protocols for paraffin embedding, submit samples to a vendor for processing, embedding, and slicing/slide mounting. Section tissues at 5 µm.
   NOTE: Due to excess adipose surrounding gland, consider removing 100-200 µm of tissue before sectioning and staining.

## 2. Tissue Staining

1. **Immunohistochemistry**
   1. Place slides to be stained on heat block set at 58 ˚C for 1 h to melt paraffin.
      CAUTION: Melting paraffin wax may run off slide. Monitor closely or place wipe under slide to capture runoff wax.
      NOTE: This step is not essential and may be skipped. If results are not as expected, adding this step back may improve results.
   2. Incubate slides in a slide jar containing 100% xylene for 30 min ensuring complete submersion. Repeat once.
      NOTE: At this point, visual inspection should be performed to ensure that tissue sections are free of adipose tissue and paraffin. If additional adipose tissue or wax is evident, the slide should be re-submerged in xylene. Use caution to minimize added exposure to xylene as this can cause shrinkage of the tissue.
   3. Rehydrate tissues in a slide jar containing 100% ethanol for 10 min. Repeat once.
   4. Move slides to a slide jar containing 95% ethanol for 10 min. Repeat once.
   5. Move slides to a slide jar containing 75% ethanol for 5 min.
   6. Move slides to a slide jar containing 50% ethanol for 5 min.
   7. Boil 10 mM sodium citrate solution (pH 6.0) in a hot plate or a microwave and pour into Coplin jar.
      CAUTION: Carefully monitor solution while heating and take care to avoid boil over. Container will be very hot. Use protection to avoid burns.
   8. Slowly place slides into Coplin jar, ensuring complete submersion, and incubate at 100 °C for 10 min to retrieve epitopes. Remove and carefully dry slides.
   9. Draw a barrier around tissue with a hydrophobic marker.Add enough endogenous enzyme blocker (hydrogen peroxide and sodium azide, available commercially) to cover tissue and incubate for 10 min.
   10. Submerge slides in 1x phosphate buffered saline (PBS) for 10 min.
   11. Add enough 10% donkey serum in 1x PBS to cover tissue and incubate for 1 h at room temperature in a humidified chamber.
       NOTE: The experiment can be paused here by storing the slides in the humidified chamber at 4 °C overnight. While donkey serum was found to yield optimal staining results, the investigator may wish to test different sera such as bovine serum albumin (BSA), goat serum or horse serum to determine optimal results. If using BSA, the investigator should prepare this fresh before use.
   12. Decant excess blocker from slides and add properly diluted primary antibody in 1% serum directly to slides ensuring that the tissue is evenly covered in solution. Incubate for 30 min at room temperature in a humidified chamber.
       NOTE: This step may be continued for longer time durations with humid chamber stored at 4 °C. Make sure to include proper negative control slides (*e.g.* a slide with no primary antibody, known antigen-negative tissue, *etc.*) at this step.
   13. Carefully wash slides by flowing about 1 mL of di$H_2O$ over tissue and incubate in 1 change of 1x PBS for 5 min.
   14. Decant excess PBS and add enough horseradish peroxidase label to cover tissue and incubate for 30 min in a humidified chamber.
       NOTE: At this step, the investigator may wish to proceed to fluorescent staining using fluorescently conjugated secondary antibodies. If this is desired, the next steps described should be modified accordingly.
   15. Carefully wash slides by flowing about 1 mL of di$H_2O$ over tissue and incubate in 1 change of 1x PBS for 5 min.
   16. Make diaminobenzidine (DAB) plus chromogen solution according to the manufacturer suggested ratio and mix by vortex.
       NOTE: Many ready-made kits are commercially available aside from the one used in this protocol.
   17. Decant excess buffer from slides and add 2-3 drops (10-50 µL) of chromogen stain directly to tissues and incubate for 5 min in humid chamber. Carefully wash slides by flowing about 1 mL di$H_2O$ over tissue.

CAUTION: DAB-chromogen is highly toxic. Avoid direct contact of stain with skin and collect flow off in hazardous waste.

2. **Hematoxylin and Eosin (H&E)**
    1. Following final rinse after chromogen incubation, submerge slides in Harris hematoxylin for 2-2.5 min. Rinse slides gently under tap water for 1-2 min.
    NOTE: Take care to avoid direct jet of water onto tissues.
    2. Submerge slides for 2-3 s in differentiation solution (0.25 mL of hydrochloric acid in 100 mL of 70% ethanol). Rinse slides gently under tap water for about 1-2 min.
    3. Submerge slides in blue agent (4.5 mg calcium carbonate in 100 mL tap water, pH adjusted to 9.4) for 60 s. Rinse slides in 95% ethanol for 30 s.
    4. Submerge slides in alcoholic eosin Y for 2-3 min.
    5. Dehydrate tissue in 2 changes of 95% ethanol for 1 min each.
    6. Dehydrate tissue in 1 change of 100% ethanol for 1 min.
    7. Carefully dry slides with a lint-free wipe. Apply 1 drop (about 100-200 µL) of synthetic, non-aqueous, resin-based mounting media to slide and apply coverslip.
    NOTE: If a different staining method was elected, a different mounting media may be required. For instance, if the investigator chose a fluorescent-conjugated secondary antibody, an aqueous mount would be more ideal.
    8. Allow slides to set overnight at room temperature.

3. **Picrosirius Red (PSR) Staining**
    1. Select slides to be stained and follow immunohistochemistry protocol through step 6 (50% ethanol soak).
    2. Submerge slides in PSR stain for 1 h.
    3. Submerge slides in 0.5% acetic acid for 1-2 s, twice to differentiate stain.
    4. Dehydrate tissues in 2 changes of 95% ethanol for 1 min each.
    5. Dehydrate tissues in 1 change of 100% ethanol for 1 min.
    6. Clear slides by briefly submerging in 100% xylene for about 3-4 s.
    7. Carefully dry slides with a lint-free wipe. Apply 1 drop (about 100-200 µL) of synthetic, non-aqueous, resin-based mounting media to slide and apply coverslip.

## 3. Sample Analysis

1. **Ductal Analysis**
    1. Select slides stained for α-SMA. Using a light microscope fitted with a camera-mounted objective, collect representative images at 20X magnification.
    2. Using ImageJ (NIH), distinguish and count ducts in each image. These can be enumerated manually or one may assign a numerical score to individual ducts. To assign a numerical score, open ImageJ and select Plugins. Next select Analyze and choose Cell Counter from the drop down menu. Click Initialize then highlight Type 1 to begin labeling ducts. When finished, select Results to view the ductal count.
    NOTE: Take care to verify structures are ductal and not vascular.
    3. In 'Set Measurement' options, check 'Perimeter' and 'Area".
    4. Using the freehand polygon tool, draw a line around each duct at the myoepithelial compartment (visibility aided by α-SMA stain). Select 'Measure' and record the perimeter and area.
    5. Again using the freehand polygon tool, draw a line along the apical side of the ductal epithelium within the interior of the lumen. Select 'Measure' and record the perimeter and area.
    6. Subtract the perimeter of the luminal compartment from the perimeter of the myoepithelial compartment in order to obtain the circumference of the ductal epithelium. Subtract the area of the luminal compartment from the area of the myoepithelial compartment to obtain the area of the ductal epithelium.

2. **Immunohistochemistry Analysis**
    1. Upload brightfield images to an analytical software, such as ImageJ or FIJI Suite.
    NOTE: This protocol outlines the steps for staining analysis using ImageJ and the IHC Toolbox plugin.
    2. Open the IHC Toolbox from the Plugin menu. In the "Select Model" combo box that opens, select appropriate stain (*i.e.* H-DAB, PSR, *etc.*). Select the "Color" option to isolate the stain. This will open a result window.
    NOTE: This method is appropriate if a protein of interest is located in the extracellular or cytosolic spaces, or is bound to the plasma membrane. If the protein of interest is nuclear, selecting "Nuclei" will prompt the plugin to analyze the image for positively stained nuclei.
    3. Use the Color Chooser Slide to ensure proper isolation of the stain without background inclusion or excessive stain exclusion.
    NOTE: If the automatic mode is unable to detect the stain or does not result in acceptable images, draw a square Region of Interest (ROI) over an identified stained region. On the IHC Toolbox window, select "Train" to direct the plugin to the appropriate target.
    4. Convert the image to 16-bit. Go to **Image → Type → 16 bit.**
    5. Threshold the image. Go to **Image → Adjust → Auto Threshold.**
    6. Set the image measurement scale by drawing a line ROI directly over the scale bar in the image then assigning the length. To set the scale bar, go to **Analyze → Set Scale.** Input the number of pixels per the desired unit of length (*e.g.* 120 pixels per 50 µm).
    7. Measure the resultant area and mean grey value. Go to **Analyze → Set Measurements** and collect the measurement by clicking **Analyze → Measure.**

## Representative Results

Female mice have 5 pairs of mammary glands. Specifically, there is one pair of cervical glands (#1), two pairs of thoracic glands (#2 and #3), one pair of abdominal glands (#4), and 1 pair of inguinal glands (#5) (**Figure 1A**). Here, we isolated the #4 glands as they are readily identifiable. In some circumstances, both #4 and #5 glands were isolated together as distinction between the two was difficult. To isolate intact #4 abdominal mammary glands, the pelt was pinned and carefully separated from the underlying peritoneum, revealing the location of the #4 glands indicated by an arrow (**Figure 1B**). The #4 glands were carefully excised and inspected for the presence of any residual subcutaneous or muscle tissue. Although these were not identifiable in our isolated glands (**Figure 1C**), we did note substantially more subcutaneous tissue in fibronectin-stained glands from tissue blocks in which tissue had not been removed prior to sectioning (*e.g.* superficial) (**Figure 1D**) versus glands in which 100-200 µm of tissue from the tissue block had been removed prior to sectioning (*e.g.* deep) (**Figure 1E**). To gain a better understanding of tissue fibrosis in the mammary gland in response to exogenous or endogenous factors, the investigator may wish to compare fibrosis in superficial versus deep cuts of the gland. For other analyses, it may be advantageous for the investigator to section the tissue block in half before proceeding to tissue slicing and staining if substantial subcutaneous and/or muscle tissue is present following gland dissection.

Following isolation, glands were fixed in 10% neutral buffered formalin, processed and sectioned for staining. The steps used for analyzing collagen expression in addition to other proteins of interest are depicted in **Figure 2A**. Representative samples from the ECM proteins collagen, fibronectin and tenascin-C are shown in **Figure 2B**. Arrows in each of the images show the presence of ducts in these tissues (**Figure 2B**).

To quantify morphological features of ducts, it is important to treat the histological sections with care as improper handling may result in damaged tissues and ducts that are not measurable. Examples of improper handling may be running buffers or water directly on the tissues, using buffers at an improper temperature or leaving tissue samples in harsh buffers such as sodium citrate and acetic acid for a longer period of time than specified in the protocol. An example of a tissue section in which tissue damage has occurred is shown in **Figure 3A**. Here, extensive damage to the tissue can be readily observed as breakage points in the ducts (**Figure 3A**). A section such as this cannot be used for analyses of ductal structures. An example of an intact tissue specimen where the ducts are measurable and quantifiable is shown in **Figure 3B**. Here, the ducts are not only characterized by the surrounding fibronectin-stained stroma, but are also characterized by the presence of a dense population of epithelial cells lining the lumen of the ducts (**Figure 3B**). It is important to note that during development, the mouse mammary gland contains a single duct at birth from which lateral secondary branches sprout, forming a more complicated ductal tree which undergoes a series of branching and regression with each estrous cycle [13]. Although we have not taken into consideration the estrous cycle of the animals in these experiments, the investigator may wish to do so in order to obtain information on ductal numbers independent of the estrous cycle. The investigator is referred to a protocol by Caligioni[14] in which the stage of the estrous cycle can be visibly determined. With regard to quantifying ducts, the presence of multiple ductal structures in these histological sections is not indicative of multiple unique ducts, but is rather indicative of a more developed ductal tree resulting from ductal outgrowth. To enumerate ducts, one may use an image analysis software such as ImageJ (NIH) to assign a number to individual ducts in a tissue section. The investigator may wish to enumerate ducts as alterations in ductal numbers, which may be indicative of developmental abnormalities or a pathological condition. With respect to our study, we believe the increased number of ducts, a result of ductal outgrowth, is related to the loss of caveolin-1 which may drive the aberrant expression of growth factors such as insulin growth factor 1 (IGF-1), a known mediator of mouse ductal growth [15].

In addition to the presence of intact ducts, several ducts contain branches, indicated by arrows in a fibronectin-stained section (**Figure 3C**). For the purpose of this analysis, these ductal branches should not be considered as a separate ductal structure. While evaluating and measuring ducts, it is important to distinguish ducts from vascular structures. Vascular structures can not only be identified by the presence of an endothelial monolayer lining the lumen, but also by the presence of a-nuclear, eosinophilic structures indicative of red blood cells (RBC) within the lumen (**Figure 3D**). Although the presence of eosinophilic structures within lumens indicates RBC and suggests vasculature, the displacement of RBC during gland collection throughout tissue sections is possible. It is advisable to confirm vascular structures using the endothelial marker CD31. An example of a histological section stained with CD31 is shown (**Figure 3D**). In order to quantify ductal circumference and area, vectors in ImageJ (NIH) can be assigned to outline the myoepithelial border (circumference) and the luminal border in α-SMA-stained tissue section. α-SMA, a marker of smooth muscle cells, was used as it stains the myoepithelial cells which line ducts. In the image shown, the red line shows the myoepithelial border while the blue line shows the luminal border (**Figure 3E**). The region between the stromal and luminal compartments, shown in the schematic, is the area occupied by the total stromal tissue plus the ductal epithelial cells (**Figure 3E**).

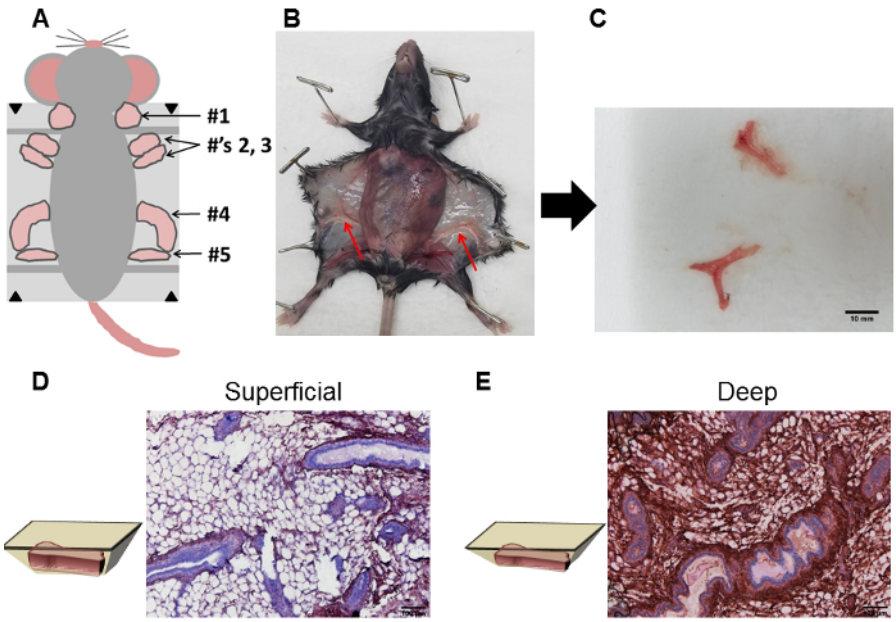


**Figure 1: Isolation of whole, intact mammary glands for histological analyses. (A)** Following animal sacrifice, the pelt was carefully removed and pinned back to expose the mammary glands located between the dermis and peritoneum. The schematic shows the relative positions of the cervical (#1), thoracic (#'s 2 and 3), abdominal (#4) and inguinal (#5) glands. **(B)** The #4 abdominal glands, shown in the dissected animal and indicated by the red arrows, were isolated. **(C)** Representative example of #4 abdominal glands isolated from a nulliparous female B6 mouse. **(D)** Substantial subcutaneous tissue from glands in which tissue had not been removed from the paraffin block prior to sectioning (*e.g.* superficial) was apparent following staining for the ECM protein fibronectin. **(E)** Considerably less subcutaneous tissue and more fibronectin stained stromal tissue were observed from glands in which 100-200 µm of tissue had been removed from the paraffin block prior to sectioning (*e.g.* deep). Histological sections are from representative samples. Please click here to view a larger version of this figure.

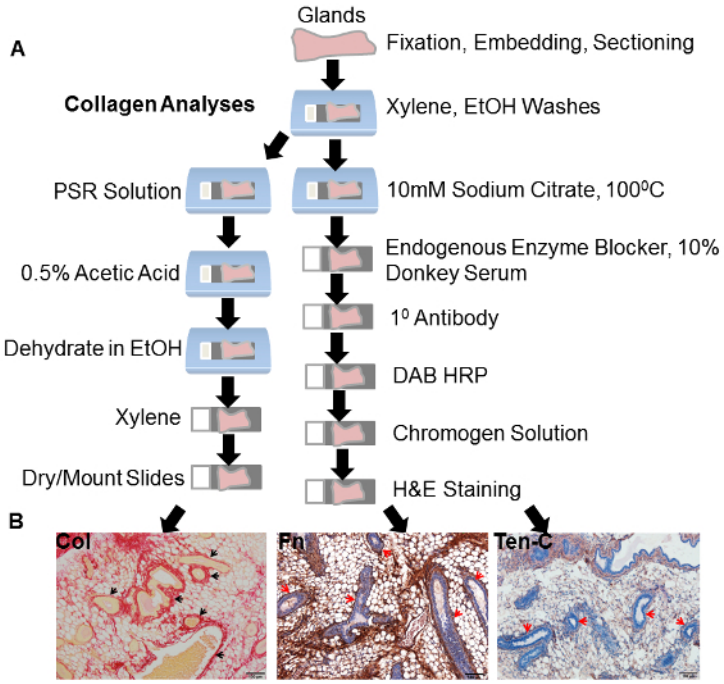


**Figure 2**: **Histological processing and staining. (A)** Schematic representation of the steps used for histological processing. A different series of steps was utilized for analyses of collagen expression. **(B)** Representative images of the ECM proteins collagen, fibronectin and tenascin-C from the glands of female nulliparous caveolin-1 deficient animals. Arrows for collagen, fibronectin and tenascin-C indicate the dense stroma lining the ducts. PSR: Picrosirius Red. Fn: fibronectin. Ten-C: tenascin-C. Please click here to view a larger version of this figure.

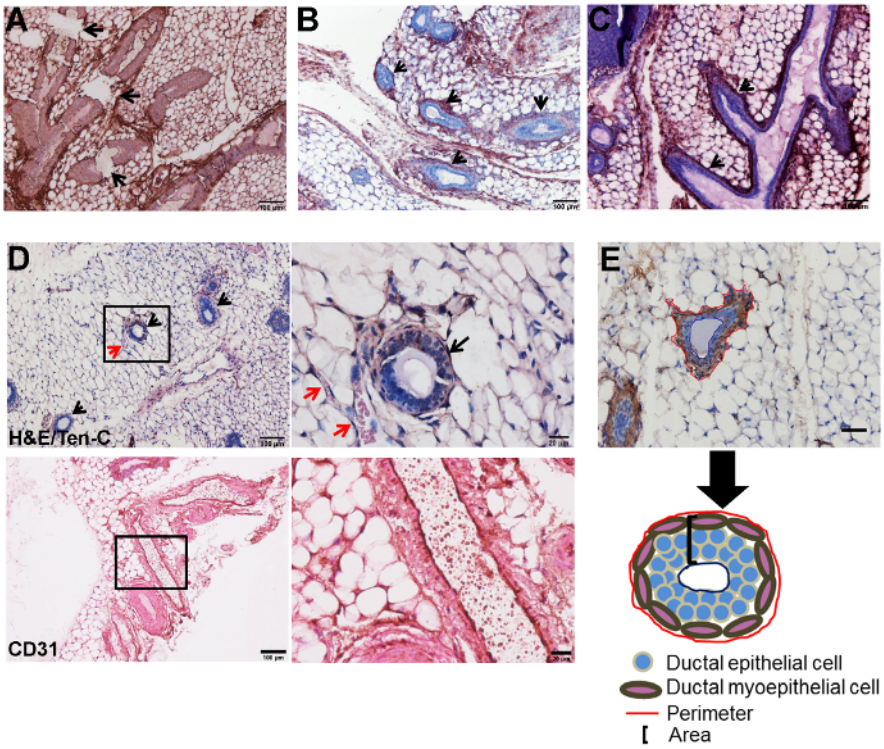


**Figure 3**: **Analyses of ductal architecture. (A)** A fibronectin stained section illustrates extensive tissue damage. This is marked by the presence of breaks in the ductal structures (arrows). **(B)** A fibronectin stained section illustrates the presence of intact ductal structures which are marked by the presence of lumens surrounded by one or more layers of epithelial cells and a surrounding stroma. Arrows indicate individual ductal structures. **(C)** A fibronectin-stained image highlights the presence of ductal branches, which are indicated with arrows. Note the continuity of these with the lumen of the larger ductal structure. **(D)** Vascular structures (red arrows), characterized by a single layer of cells and the presence of a-nucleated eosinophilic structures indicative of red blood cells, are frequently observed in proximity with the ducts (black arrow). Low magnification is shown in the image on the left and a corresponding high magnification image is shown on the right. These images were stained with H&E and tenascin-C. CD31 was used as a positive marker for the endothelial cells lining the vascular structures. Shown is a large vascular structure in which CD31 positive cells are visible lining the lumen of the vessel. Low magnification is shown in the image on the left and a corresponding high magnification image is shown on the right. **(E)** Ductal circumference was measured in an α-SMA-stained image using a vector (shown in red) to outline the myoepithelial compartment while ductal area was measured using a vector (shown in blue) to outline the luminal compartment. The region in between the stromal and luminal compartments was classified as the ductal area. Scale bar = 50 µm. Schematic of a ductal structure highlighting the areas from which the perimeter and area were measured. Ten-C: tenascin-C. The histological section in Figure E was modified from: Thompson C *et al.*[16] Please click here to view a larger version of this figure.

## Discussion

In the paper, we have described a technique to isolate intact mouse mammary glands for downstream histological analyses of ECM expression and ductal morphology. With respect to analyses of ductal morphology, this methodology enables the rapid investigation of ductal architecture based off of stained histological sections. Other methods of ductal analyses rely on injections of dyes to enable visualization of the ductal tree, methods which may be technically challenging and time consuming.

In breast cancer, the ECM has been reported to be abnormal.[1,2,6,9] Specifically, changes in the abundance and/or cross-linking patterns of the ECM have been reported to influence tumor progression, metastasis and therapy resistance[3,4,6,7,8,9]. In addition, changes in the ECM milieu have also been reported to alter ductal epithelial cell morphology and proliferation[17], potentially leading to a situation favoring tumor initiation. While we utilized a caveolin-1 deficient animal model to assess changes in ECM expression and ductal morphology following loss of caveolin-1, one may apply this methodology in any mouse model. To assess ECM expression patterns and ductal architecture, we describe a technique to isolate whole, intact mammary glands for downstream histological analyses. Results from this methodology yielded robust analyses of ECM expression and glandular morphology. We found that analyzing ECM expression, especially fibronectin, from sections in which 100-200 µm of superficial tissue was removed prior to sectioning and staining yielded a more complete picture of glandular fibrosis. Additionally, we found that use of donkey serum as opposed to BSA yielded better quality histological samples in which non-specific staining was substantially reduced.

For analyses of ductal architecture, it is important to use sections in which tissues are intact and contain ducts in which breakage points, a result of improper tissue handling and sectioning, are not evident. Furthermore, it is important to correctly distinguish ductal branches, another parameter that an investigator may wish to measure, and vascular structures which can easily be identified by their monolayer endothelium and eosinophilic structures within the lumen in addition to staining with CD31. While ducts were observed in sections stained for various ECM proteins, the myoepithelial marker αSMA and H&E counterstaining, which highlighted the cellular component of the ducts, enumeration of ducts and any associated branches is achievable with H&E stained tissue sections alone. For more detailed analyses of ductal morphogenesis or analyses of the presence of pre-neoplastic and/or neoplastic lesions, an investigator may wish to utilize confocal imaging to evaluate live *ex-*

*vivo* tissues. In this instance, the same technique in which whole glands are excised can be applied with the fixation and tissue processing steps eliminated.

Critical steps in this protocol include the use of surgical micro loupes which not only enabled the precise identification of the #4 abdominal glands, but additionally permitted the dissection of the gland from the overlying dermis and underlying peritoneum. The exclusion of substantial subcutaneous tissues and muscles reduced adipose-associated interference in staining and histology. In addition, to better identify ECM expression changes in the gland, we found it useful to remove 100-200 µm of the tissue block, which helped eliminate residual adipose tissue. Although whole mammary gland isolation provides information on tissue wide changes in stromal protein expression and ductal morphogenesis, the described technique is limited to analysis of serial sections from fixed, paraffin embedded tissues. To establish the degree to which changes in ductal branching have occurred, whole mount imaging of live, *ex-vivo* tissues would be necessary. Here, an investigator could use Cre-Lox to design custom, conditional fluorescent reporter conjugations to study gland specific protein interactions or utilize a dye to illuminate the ductal tree prior to imaging[18]. In addition to this, further analysis of proteins of interest in the entirety of the gland would necessitate the use of western blot or mass spectrometry or other high-throughput techniques such as cross-linking immunoprecipitation (CLIP) or chromatin immunoprecipitation (ChIP). In this instance, whole glands would be dissected, sectioned into small pieces and processed accordingly for the downstream analyses. In addition, one may also use fluorescent imaging on tissue sections. This technique would be ideal for analyzing multiple proteins and protein expression co-localization in the same tissue.

In summary, we describe a technique that offers the rapid isolation of whole, intact mammary glands and provides further details on histological processing and ductal analyses. Future applications of this technique could investigate ECM expression and associated changes in ductal morphology in tumor-bearing animals. Furthermore, analyses of collagen orientation and fiber diameter, information which may be useful for analyzing tissue density, may also be performed on PSR stained sections.

## Disclosures

The authors have nothing to disclose.

## Acknowledgements

The authors would like to acknowledge April Wiles and Dr. Roger Broderson for assistance with animal necropsy and gland isolation, respectively. Funding for this work was supported by the Philadelphia College of Osteopathic Medicine Centers for Chronic Disorders of Aging.

## References

1. Gao-Feng Xiong, R. X. Function of cancer cell-derived extracellular matrix in tumor progression. *J Cancer Metastasis Treat.* **2,** 357-364 (2016).
2. Place, A. E., Jin Huh, S., & Polyak, K. The microenvironment in breast cancer progression: biology and implications for treatment. *Breast Cancer Res.* **13** (6), 227 (2011).
3. Provenzano, P. P. *et al.* Collagen reorganization at the tumor-stromal interface facilitates local invasion. *BMC Med.* **4** (1), 38 (2006).
4. Provenzano, P. P. *et al.* Collagen density promotes mammary tumor initiation and progression. *BMC Med.* **6** 11 (2008).
5. Cox, T. R., & Erler, J. T. Remodeling and homeostasis of the extracellular matrix: implications for fibrotic diseases and cancer. *Dis Model Mech.* **4** (2), 165-178 (2011).
6. Ioachim, E. *et al.* Immunohistochemical expression of extracellular matrix components tenascin, fibronectin, collagen type IV and laminin in breast cancer: their prognostic value and role in tumour invasion and progression. *Eur J Cancer.* **38** (18), 2362-2370 (2002).
7. Barkan, D. *et al.* Metastatic growth from dormant cells induced by a col-I-enriched fibrotic environment. *Cancer Res.* **70** (14), 5706-5716 (2010).
8. Levental, K. R. *et al.* Matrix crosslinking forces tumor progression by enhancing integrin signaling. *Cell.* **139** (5), 891-906 (2009).
9. Wang, J. P., & Hielscher, A. Fibronectin: How Its Aberrant Expression in Tumors May Improve Therapeutic Targeting. *J Cancer.* **8** (4), 674-682 (2017).
10. Qian, N. *et al.* Prognostic significance of tumor/stromal caveolin-1 expression in breast cancer patients. *Cancer Sci.* **102** (8), 1590-1596 (2011).
11. Simpkins, S. A., Hanby, A. M., Holliday, D. L., & Speirs, V. Clinical and functional significance of loss of caveolin-1 expression in breast cancer-associated fibroblasts. *J Pathol.* **227** (4), 490-498 (2012).
12. Witkiewicz, A. K. *et al.* An absence of stromal caveolin-1 expression predicts early tumor recurrence and poor clinical outcome in human breast cancers. *Am J Pathol.* **174** (6), 2023-2034 (2009).
13. Macias, H., & Hinck, L. Mammary gland development. *Wiley Interdiscip Rev Dev Biol.* **1** (4), 533-557 (2012).
14. Caligioni, C. S. Assessing reproductive status/stages in mice. *Curr Protoc Neurosci.* **Appendix 4** Appendix 4I (2009).
15. Cannata, D. *et al.* Elevated circulating IGF-I promotes mammary gland development and proliferation. *Endocrinology.* **151** (12), 5751-5761 (2010).
16. Thompson, C., Rahim, S., Arnold, J., & Hielscher, A. Loss of caveolin-1 alters extracellular matrix protein expression and ductal architecture in murine mammary glands. *PLoS One.* **12** (2), e0172067 (2017).
17. Williams, C. M., Engler, A. J., Slone, R. D., Galante, L. L., & Schwarzbauer, J. E. Fibronectin expression modulates mammary epithelial cell proliferation during acinar differentiation. *Cancer Res.* **68** (9), 3185-3192 (2008).
18. Krause, S., Brock, A., & Ingber, D. E. Intraductal injection for localized drug delivery to the mouse mammary gland. *J Vis Exp.* (80) (2013).

 